Princeton Plasma Physics Laboratory

NSTX Experimental Proposal

Title: Dependence of ELM size and Power Balance on drsep

OP-XP-609	**Revision:**	Effective Date: 03/08/06 *(Ref. OP-AD-97)* Expiration Date: *(2 yrs. unless otherwise stipulated)*

PROPOSAL APPROVALS

Author: R. Maingi	Date
ATI – ET Group Leader: R. Maingi	Date
RLM - Run Coordinator: R. Raman (S. Sabbagh)	Date

Responsible Division: Experimental Research Operations

Chit Review Board (designated by Run Coordinator)

MINOR MODIFICATIONS (Approved by Experimental Research Operations)

Comment from Run Coordinator: consider running this close to XP #525 (dependence of ELMs on κ and δ) to minimize development time.

NSTX EXPERIMENTAL PROPOSAL

Dependence of ELM size and Power Balance on drsep **OP-XP-609**

1. Overview of planned experiment

The primary goal of this experiment is to measure the transition point(s) from small ELMs to large ELMs as a function of the magnetic balance as characterized by the EFIT δ_r^{sep} parameter. The secondary goal is to measure the dependence of the up/down divertor power balance split on magnetic balance.

2. Theoretical/ empirical justification

Projections[1] of the energy loss from Type I ELMs for the International Thermonuclear Experimental Reactor (ITER) have yielded a pedestal energy loss fraction between 5% and 20%, depending on the model used for extrapolation. Here the pedestal energy loss fraction is given by $\Delta W/W_{ped}$, where ΔW is the stored energy change during the ELM and W_{ped} is the stored energy in the H-mode pedestal. Figure 1 shows the extrapolation for Type I ELMs assuming ELM power carried by ions flowing at the ion sound speed in the scrape-off layer, which yields a prediction of 4-12% for ITER. Figure 2 shows the dependence of ELM power loss on collisionality at the top of the pedestal ν^*; it is seen that $\Delta W/W_{ped} \sim 20\%$ for the predicted ITER ν^*. The power loading problem in ITER would be greatly simplified by the elimination of ELMs with resonant magnetic perturbations[2] or by access to small ELM regimes.

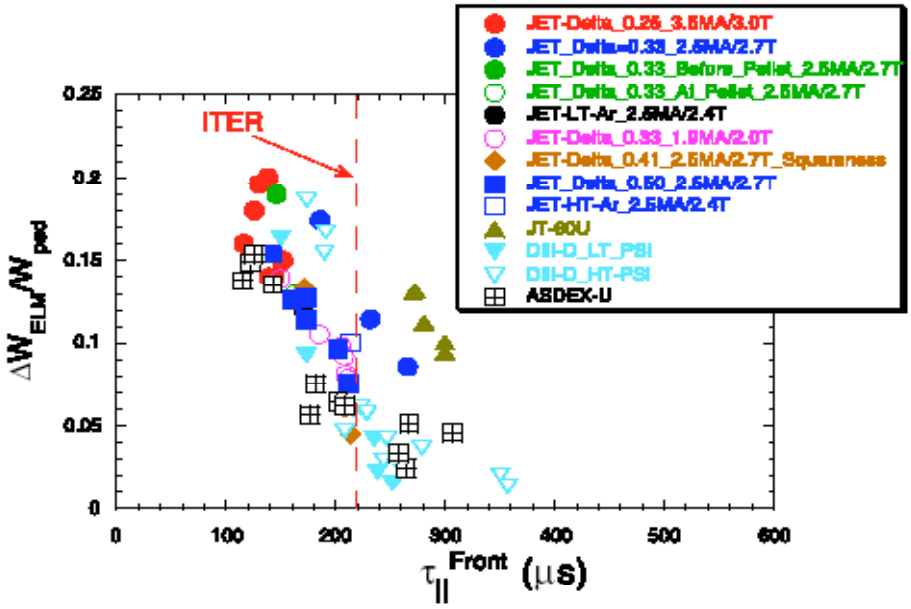

Figure 19. Normalized ELM energy loss ($\Delta W_{ELM}/W_{ped}$) versus SOL ion flow parallel time calculated for the pedestal plasma parameters ($\tau_{||}^{Front}$), for a large range of Type I ELMy H-mode plasmas in ASDEX Upgrade, DIII-D, JT-60U and JET including various plasma triangularities, ratios of P_{INPUT} to P_{L-H}, impurity seeding (Ar) and pellet triggered ELMs.

Fig. 1 from reference[1], where extrapolation to ITER is done via a physics-based model assuming ELM power flow on the open field lines at the ion sound speed.

We have identified[3] a small ELM regime in NSTX, named Type V ELMs to distinguish them technically from Type II and grassy ELMs seen on other devices. These ELMs were observed in lower triangularity $\delta \sim 0.4$ discharges, when the $\delta_r^{sep} \leq -1$cm. Note that the convention for δ_r^{sep} is negative (positive) when the lower (upper) X-point is favored; a balanced double-null has $\delta_r^{sep} \sim 0$. When the discharge was changed to a balanced double-null, Type I and III ELMs were observed. In the LSN configuration, large Type I ELMs between the Type V ELMs were observed when $\nu^* \leq 1$ which also corresponded to $\beta_N \geq 5$.

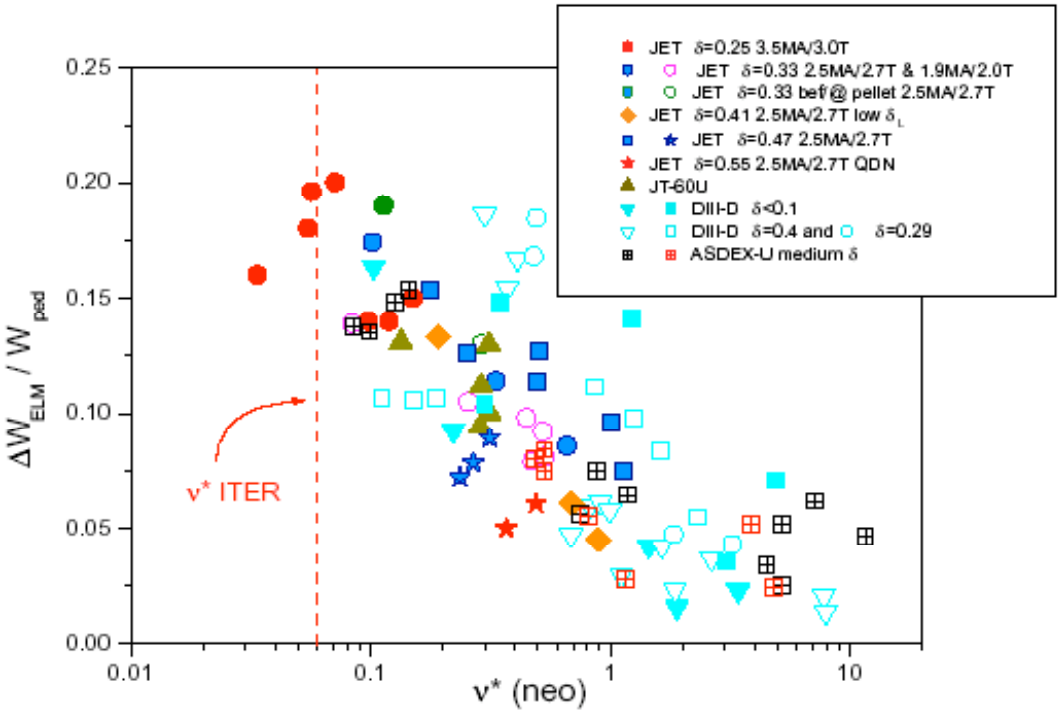

Figure 11. Normalized ELM energy loss ($\Delta W_{ELM}/W_{ped}$) versus pedestal plasma collisionality for a large range of Type I ELMy H-mode plasmas in ASDEX Upgrade, DIII-D, JT-60U and JET including various plasma triangularities, ratios of P_{INPUT}/P_{L-H} and pellet triggered ELMs.

Fig. 2 from reference[1], where 'extrapolation' to ITER is based solely on pedestal ν^*.

In more recent high $\delta \sim -0.75$ discharges, a small ELM regime was observed when δ_r^{sep} was ~ -0.5cm, and large Type I ELMs were observed with $\delta_r^{sep} \sim 0$. These small ELMs appeared similar to Type V ELMs on several diagnostics, except perhaps with toroidal mode number $n > 1$. The observed pedestal temperature was higher in this shape, leading to a pedestal $\nu^* \sim 0.3$, and yet no Type I ELMs were observed. Thus, it is evident the plasma shape plays an important role in determining the boundaries between large and small ELMs.

To give confidence in edge stability predictions for ITER, the boundary between small ELMs and large ELMs should be measured experimentally and simulated. In particular, any dependencies which extend the operating range of small ELM regimes, e.g. high δ, to more ITER-like parameters, e.g. ν^*, should be a near term focus. This is the focus of this experiment.

In addition, we will measure the power balance as a function of δ_r^{sep} in piggyback mode, to complete our previous study[4], in which we inferred an improved power accountability in DN discharges as compared with LSN discharges.

3. Experimental run plan (1 day, prioritized list below)

Perform δ_r^{sep} scan in high d~ 0.75

- Reproduce rtEFIT long pulse #119085 with δ_r^{sep} ~ -0.5 cm (2)
- Do a δ_r^{sep} ramp from 0 to -3 cm and back down to 0 (2)
- Increase δ_r^{sep} in 0.2 cm steps from –0.5 cm until H-mode lost (5)
- Reproduce baseline #119085 (1)
- Decision point: Perform δ_r^{sep} scan at -1.0 cm, -1.5 cm, -2 cm, -2.5 cm until H-mode lost and/or ELMs change substantially or do a binary search to find δ_r^{sep} window for small ELMs (6)
- Time permitting, localize δ_r^{sep} value if/when ELMs change or H-mode lost as δ_r^{sep} decreases (4)

Perform δ_r^{sep} scan for PF2L LSN with low δ ~ 0.4

- Reproduce rtEFIT #119136 with δ_r^{sep} ~ -2 cm, add 3rd NBI src and increase to 0.8 MA (3)
- Do a δ_r^{sep} ramp from -2 to 0 cm and back to -3 cm (2)
- Decision point: Perform δ_r^{sep} scan at 0 cm, -0.5 cm, -1 cm, -1.5 cm or do a binary search to find δ_r^{sep} window for small ELMs (4)
- Localize δ_r^{sep} when ELMS change (4)

4. Required machine, NBI, RF, CHI and diagnostic capabilities

This XP requires an operational NBI system, as well as the capability of performing a detailed δ_r^{sep} scan with rtEFIT. We desire HeGDC between shots of ~ 6.5 minutes for a 12.5 minute repetition rate.

5. Planned analysis

Edge stability calculations will be done with a number of codes, including PEST, DCON, and ELITE, and possibly MARS. The power balance will be compared to calculations with simple 2-point and 1-D models.

6. Planned publication of results

Data and analysis will be presented at ITPA pedestal and SOL group meetings and published in Nucl. Fusion.

PHYSICS OPERATIONS REQUEST

Dependence of ELM size and Power Balance on drsep **OP-XP-609**

Machine conditions (specify ranges as appropriate)

I_{TF} (kA): **52** Flattop start/stop (s): _____/_____

I_P (MA): **0.8-1.0** Flattop start/stop (s): **0.15/1.5 (max)**

Configuration: **Lower Single Null / Upper SN / Double Null**

Outer gap (m): **5-15cm**, Inner gap (m): **2-10cm**

Elongation κ: **1.8-2.3**, Triangularity δ: **0.4-0.8**

Z position (m): **0.00**

Gas Species: **D**, Injector: **Inner wall Midplane**

NBI - Species: **D**, Sources: **A/B/C**, Voltage (kV): **90**, Duration (s): **<1.5 sec**

ICRF – Power (MW): ____, Phasing: , Duration (s): _____

CHI: **Off**

Either: List previous shot numbers for setup: **119085 (DN), 119136 (LSN)**

Or: Sketch the desired time profiles, including inner and outer gaps, κ, δ, heating, fuelling, etc. as appropriate. Accurately label the sketch with times and values.

DIAGNOSTIC CHECKLIST

Dependence of ELM size and Power Balance on drsep OP-XP-609

Diagnostic	Need	Desire	Instructions
Bolometer - tangential array	✓		
Bolometer array - divertor	✓		
CHERS	✓		
Divertor fast cameras		✓	
Dust detector			
EBW radiometers			
Edge deposition monitor		✓	
Edge pressure gauges		✓	
Edge rotation spectroscopy		✓	
Fast lost ion probes – IFLIP		✓	
Fast lost ion probes – SFLIP		✓	
Filtered 1D cameras		✓	
Filterscopes	✓		
FIReTIP	✓		
Gas puff imaging		✓	
High-k scattering			
Infrared cameras	✓		
Interferometer – 1 mm			
Langmuir probes - PFC tiles		✓	
Langmuir probes - RF antenna			
Magnetics – Diamagnetism	✓		
Magnetics – Flux loops	✓		
Magnetics – Locked modes	✓		
Magnetics – Pickup coils	✓		
Magnetics - Rogowski coils	✓		
Magnetics - RWM sensors	✓		
Mirnov coils – high frequency	✓		
Mirnov coils – poloidal array	✓		
Mirnov coils – toroidal array	✓		
MSE	✓		
Neutral particle analyzer		✓	
Neutron Rate (2 fission, 4 scint)			
Neutron collimator			
Plasma TV	✓		
Reciprocating probe		✓	
Reflectometer - FM/CW		✓	
Reflectometer - fixed frequency homodyne		✓	
Reflectometer - homodyne correlation		✓	
Reflectometer - HHFW/SOL		✓	
RF antenna camera			
RF antenna probe			
Solid State NPA			
SPRED		✓	
Thomson scattering - 20 channel	✓		
Thomson scattering - 30 channel	✓		
Ultrasoft X-ray arrays	✓		
Ultrasoft X-ray arrays - 2 color		✓	
Visible bremsstrahlung det		✓	
Visible spectrometers (VIPS)			
X-ray crystal spectrometer - H			
X-ray crystal spectrometer - V			
X-ray PIXCS (GEM) camera			
X-ray pinhole camera			

[1] A. Loarte, et. al., 2003 *Plasma Physics Controlled Fusion* **45** 1549.
[2] T. E. Evans, et. al., 2004 *Physical Review Letters* **92** article #235003.
[3] R. Maingi, et. al., 2005 *Nuclear Fusion* **45** 264.
[4] S. F. Paul, et. al., 2005 *J. Nucl. Materials* **337-339** 251.